PHYSICAL REVIEW B **69**, 115409 (2004)

Ab initio morphology and surface thermodynamics of α-Al_2O_3

Arnaud Marmier* and Stephen C. Parker†
Department of Chemistry, University of Bath, Bath BA2 7AY, United Kingdom

(Received 29 July 2003; revised manuscript received 24 November 2003; published 15 March 2004)

We apply an *ab initio* methodology to model the low index non-stoichiometric surfaces of α-alumina, namely the (0001), $(01\bar{1}\bar{2})$, $(11\bar{2}\bar{3})$, $(11\bar{2}0)$, $(10\bar{1}0)$, $(10\bar{1}\bar{1})$, and $(22\bar{4}\bar{3})$ surfaces. We express the stabilities in terms of general surface phase diagrams, which are dependent on temperature and partial pressures of oxygen and hydrogen. Thus, the stable structures and compositions can be evaluated at specific experimental conditions. We show that under ambient conditions there is a common trend, namely only two types of surfaces are thermodynamically stable except at extremes of oxygen or hydrogen partial pressures. These are either fully stoichiometric or fully hydroxylated. We also compare the relative surface stability by generating a Wulff construction. The predicted morphologies compare very well with recent measurements, with the exception of the $(10\bar{1}\bar{1})$ surface.

DOI: 10.1103/PhysRevB.69.115409 PACS number(s): 68.35.Md, 68.47.Gh

I. INTRODUCTION

Alumina (Al_2O_3) is one of the most widely used, general-purpose technical ceramic. All aluminas are very hard, wear resistant and coupled with their high compressive strength show resistance against extreme temperatures and corrosive environments. Aluminas are also excellent electrical insulators and are often used as a substrate for electronic devices or catalysts.[1,2]

As a consequence, there has been much interest in understanding the behavior of alumina surfaces. Furthermore, as high quality single crystals can be prepared, alumina is used as a model system for the study of oxide surfaces.

The most studied surface by far is the basal plane, denoted (0001) in hexagonal symmetry [(111) in rhombohedral notation]. One of the reasons is that although experiment and theory do agree that there is substantial relaxation of the surface metal ions into the bulk, they do, however, disagree significantly about the extent of the relaxation. The consequence of this disagreement is that it has triggered highly detailed experiments[3–9] and sophisticated simulations in an attempt to account for this difference in relaxations. These have included studies on the effect of the environment, the consideration of non-stoichiometric terminations[10–13] and the examination of the effect of dynamics on the average atom positions.[14,15] Nevertheless, it is still not clear whether this discrepancy is due to the fact that the surfaces probed by experiments are far from ideal, or due to an inherent weakness of the electronic structure simulation methods.

Non-basal surfaces have historically received much less attention, but this is changing, most notably by recent experiments attempting to characterize the $(11\bar{2}0)$[16] and $(01\bar{1}\bar{2})$[17] surfaces. Very few theoretical studies have considered these surfaces, and to the best of our knowledge, all have employed semiempirical modeling techniques,[18,19] with the exception of the early density functional theory (DFT) work of Gillan[20] (the study of Guo *et al.*[21] did not include surface relaxation and hence is not considered further).

An important aim of this work is to attempt to interpret and link the experimental results from both the natural environment, where the stoichiometry is poorly constrained and partial gas pressures are high, to the results from surface science experiments, where highly characterized surfaces are studied in the presence of low pressures. Therefore, a key stage is to be able to model the surface energies as a function of the gas partial pressures. In this study, we carry out non-stoichiometric, *ab initio* calculations of the energetics of different (low-index) surfaces of alumina, namely the (0001), $(01\bar{1}\bar{2})$, $(11\bar{2}\bar{3})$, $(11\bar{2}0)$, $(10\bar{1}0)$, $(10\bar{1}\bar{1})$, and $(22\bar{4}\bar{3})$ surfaces. We investigate the effect of varying the partial pressure of O_2, H_2, or H_2O in equilibrium with each surface at different temperatures, in the spirit of the seminal work of both Sheffler[10] and Finnis.[11] We can then compare the relative stability of the surfaces for different partial pressures and temperatures. To a limited extent, comparison with experiments on different surfaces also tests our confidence in the *ab initio* ability to model the surface structures reliably.

However, before discussing the results, we review the methodology used for evaluating surface energy.

II. METHODOLOGY

A. Parameters of total energy calculation

The different surfaces are first generated with the atomistic surface package METADISE[22] which uses simple shell models potential to simulate the surfaces of interest. This allows us to screen the vast number of different possible cuts for each surface and select the most likely candidate stoichiometric structures.

We then use the total energy plane wave package VASP[23–26] for all electronic structure calculations, with its implementation of the generalized gradient approximation (GGA). The bulk lattice constant is first determined, and each surface is then relaxed in slab geometry assuming constant area, starting from the ideal bulk coordinates predicted by the atomistic approach. The slabs thicknesses are chosen so that the surfaces of each side are equivalent. For most of the surfaces a relatively small 30 atoms unit cell (12 Al, 18 O) was sufficient to assure both two-dimensional (2D) periodicity and surface equivalence on each side of the slab.

The pseudopotentials for Al, O, and H are of the ultrasoft form.[27,28]

All calculations are made with a $3\times3\times1$ k point mesh (5 irreducible k-points), and with a plane wave cutoff of 300 eV. The effect on the surface energy of increasing the plane wave cutoff to 500 eV are limited to less than 1%, which we take as a satisfactory convergence/speed compromise.

B. Surface free energy for non-stoichiometric surfaces

We now present the thermodynamic formalism used to calculate the surface energies of non-stoichiometric surfaces. A reader familiar with this approach might skip parts 1 and 2.

1. Surface energy

We begin by defining the surface energy. If we consider an oxide of chemical formula A_mO_n, in chemical equilibrium with an atmosphere containing O_2, H_2, or H_2O, the oxide slab contains N_A metal atoms at chemical potential μ_A, N_O oxygen atoms at chemical potential μ_O and N_H hydrogen atoms at chemical potential μ_H.

Let us first define the oxygen excess

$$\Gamma_O=[N_O/N_A]=\frac{1}{2S}\left(N_O-\frac{n}{m}N_A\right),$$

and hydrogen excess

$$\Gamma_H=[N_H/N_A]=\frac{1}{2S}(N_H).$$

As the slab has two surfaces of area S, the total surface area is defined as $2S$.

The surface energy can be expressed as

$$\gamma_{AO}=\frac{1}{2S}(G_{AO}^{\mathrm{slab}}-N_A\mu_A-N_O\mu_O-N_H\mu_H),$$

where G_{AO}^{slab} is the Gibbs free energy of the slab.

The Gibbs energy per formula unit g_{AO} is directly related to the energy of the bulk, as calculated. Then,

$$g_{AO}=\frac{m}{N_A}G_{AO}^{\mathrm{bulk}}.$$

As the surface is in equilibrium with its bulk, the chemical potential of the metal and of oxygen must obey the following relation

$$g_{AO}=m\mu_A+n\mu_O.$$

where g_{AO} is the Gibbs energy of bulk alumina, per formula unit. The chemical potential of oxygen and aluminum are not independent.

By recombining, we obtain first

$$\gamma_{AO}=\frac{1}{2S}\left(G_{AO}^{\mathrm{slab}}-\frac{N_A}{m}g_{AO}\right)-\Gamma_O\mu_O-\Gamma_H\mu_H,$$

where the first term of the r.h.s would correspond to the "stoichiometric" part of the surface energy, since $(N_A/m)\,g_{AO}$ is the free energy of an equivalent amount of bulk material in the slab.

At this point, we assume that the entropic excess contributions to the free energy are negligible (following Refs. 11 and 10) and, therefore,

$$\gamma_{AO}=\frac{1}{2S}\left(E_{AO}^{\mathrm{slab}}-\frac{N_A}{m}e_{AO}\right)-\Gamma_O\mu_O-\Gamma_H\mu_H,$$

where E_{AO}^{slab} is the energy of the slab, and e_{AO} the energy of bulk alumina, per formula unit.

2. Range of chemical potential

The above expression for the surface free energy, while straightforward to derive, is quite meaningless. One needs to be able to relate the oxygen and hydrogen chemical potentials to physically more relevant variables, i.e., temperature and partial pressures.

First, we note that the oxygen chemical potential cannot take any value.

If the chemical potential of Al is higher than the chemical potential in Al metal form, alumina will tend to dissociate, thus imposing a bottom boundary on μ_O. This can be expressed as $\mu_A<g_A$, which is equivalent to $\mu_O>(g_{AO}-mg_A)/n$, where the Gibbs energy per formula unit g_A is taken as the calculated energy of the bulk metal e_A, here again assuming that the entropic contribution is negligible.

And at high oxygen chemical potential, molecular O_2 would start to condense at the surface, or

$$\mu_O<\tfrac{1}{2}g_{O_2},$$

where g_{O_2} is the Gibbs energy of an isolated O_2 molecule (at the temperature of interest). Evaluating the Gibbs energy of the O_2 molecule can complete this boundary calculation. For this one needs the calculated energy for the molecule using the same pseudopotential for O as in the slab calculation, as well as experimental data for the entropy, as it is not possible to neglect the vibrational terms for gases. However, the energy of the O_2 molecule is poorly reproduced by GGA, therefore, we use a cycle and additional experimental data.

The standard energy of formation of the oxide, corresponding to the following equation

$$mA^S+\frac{n}{2}O_2^G\rightarrow A_mO_n^S,$$

is

$$\Delta G_f^\circ(A_mO_n)=g_{AO}^\circ-m\mu_A^\circ-n\mu_O^\circ,$$

where the ° indicates standard conditions, i.e., temperature of 293.28 K and pressure of 1 bar. The important point here is that one cannot force μ_O to be zero (as is traditional for a pure substance), because our zero of energy is fixed by the electronic structure calculation (i.e., the energy of separated electrons and cores).

The unknown value, $\mathring{\mu}_{\mathrm{O}}$ can be then extracted from the calculated $\mathring{\mu}_{\mathrm{A}}$ and $\mathring{g}_{\mathrm{AO}}$ and from the experimentally determined $\Delta \mathring{G}_f(\mathrm{A}_m\mathrm{O}_n)$ which has a tabulated value[29] of $-376.77\ \mathrm{kcal\,mol}^{-1}$ for α-alumina at standard temperature T. Here again, for practical purposes we neglect the vibrational contribution to the chemical potentials of solids and use the 0 K energy e_{A} and e_{AO} in place of $\mathring{\mu}_{\mathrm{A}}$ and $\mathring{g}_{\mathrm{AO}}$.

In contrast to solids, the standard enthalpy and entropy for gases depends quite significantly on temperature, but one can use tabulated data[30] of enthalpy variation and entropy to obtain their value at any temperature.

Using the available tabulated data,[30] the Gibbs energy of the O_2 molecule at temperature T is the standard expression

$$g_{\mathrm{O}_2}(T) = 2\mu_{\mathrm{O}}^{\circ}(T^{\circ}) + T^{\circ}\cdot s_{\mathrm{O}_2}(T) + \Delta h_{\mathrm{O}_2}(T^{\circ},T) - T\cdot s_{\mathrm{O}_2}(T).$$

It is then easy to obtain the boundaries as

$$\frac{g_{\mathrm{AO}} - m g_{\mathrm{A}}}{n} < \mu_{\mathrm{O}} < \mu_{\mathrm{O}}^{\circ}(T).$$

3. Temperature and partial pressure dependence of the chemical potentials

An added bonus of the last manipulation is that we can now relate the chemical potential of O to the oxygen partial pressure, assuming an ideal gas

$$\mu_{\mathrm{O}} = \mathring{\mu}_{\mathrm{O}}(T) + \tfrac{1}{2}kT\log\left(\frac{P_{\mathrm{O}_2}}{P^{\circ}}\right).$$

We can now turn our attention to the case of hydrogen. There are two possibilities; either the hydrogen on the surface is in equilibrium with H_2, or H_2O, depending on the O_2 and its own chemical potentials.

If H is in equilibrium with H_2, then the situation is straightforward and

$$\mu_{\mathrm{H}} = \tfrac{1}{2} g_{\mathrm{H}_2}.$$

Of course, the energy of a H_2 molecule can only be calculated at 0 K, and must be extrapolated to the temperature of interest using tabulated data. Then the surface energy formula becomes

$$\gamma_{\mathrm{AO}} = \frac{1}{2S}\left(G_{\mathrm{AO}}^{\mathrm{slab}} - \frac{N_{\mathrm{A}}}{m} g_{\mathrm{AO}}\right) - \frac{1}{2}\Gamma_{\mathrm{H}} g_{\mathrm{H}_2} - \Gamma_{\mathrm{O}}\mu_{\mathrm{O}}.$$

In the case of equilibrium with H_2O (at high O chemical potential),

$$2\mu_{\mathrm{H}} + \mu_{\mathrm{O}} = g_{\mathrm{H}_2\mathrm{O}}.$$

Again, the Gibbs energy for the water molecule must be temperature corrected using the tabulated data.

The surface energy is now

$$\gamma_{\mathrm{AO}} = \frac{1}{2S}\left(G_{\mathrm{AO}}^{\mathrm{slab}} - \frac{N_{\mathrm{A}}}{m} g_{\mathrm{AO}}\right) - \frac{1}{2}\Gamma_{\mathrm{H}} g_{\mathrm{H}_2\mathrm{O}} - \left(\Gamma_{\mathrm{O}} - \frac{\Gamma_{\mathrm{H}}}{2}\right)\mu_{\mathrm{O}}.$$

Notice the change in the μ_{O} coefficient.

III. SURFACES CONSIDERED

We chose to consider the following eight low index surfaces: (0001), $(11\bar{2}0)$, $(01\bar{1}2)$, $(10\bar{1}0)$, $(10\bar{1}0)$, $(10\bar{1}1)$, $(11\bar{2}3)$, and $(22\bar{4}3)$. The reasons for selecting these is that they represent a superset of all previous calculations, and they appear in the experimental morphologies,[31,32] which provides circumstantial evidence that these are the most stable surfaces. We present here a succinct summary of the current knowledge on these surfaces.

As noted previously, there is a lot of work published on the basal (0001) surface. Indeed, one of the mysteries of the surface science of alumina concerns the nature of this simple surface. Experiments and calculations differ noticeably not only in the amount of relaxation of the surface, but also (albeit to a lesser extent) in the composition of the surface (i.e., whether it is purely Al, O, or a mixture). Ion-scattering[3,8] and x-ray[4,8] experiments conclude that the surface is Al terminated although Ahn *et al.*[3] and Guenard *et al.*[4] only considered purely Al or O terminated surfaces. One of the tensor-LEED[6] analyses concluded that a 2:1 mixture of Al and O terminated terraces was the best model to fit the data. However a more recent tensor-LEED[7,9] analysis strongly favored the Al termination. The same conclusion is reached by the most recent ion scattering experiment,[8] whose authors also considered mixtures of terminations as candidates. The theoretical conclusions are more consistent: All studies, whether semiempirical[14,18] or using different flavors of *ab initio*, Hartree–Fock (HF)[33] or based on DFT,[10–12,34] identify the Al terminated surface as the most stable in ambient conditions. Note that more recent DFT work includes the effect of environment on the surface free energy in a very simple way, namely by taking into account the effect of a partial pressure of water,[12] hydrogen,[10] or oxygen.[11] In all cases, an Al terminated surface is the most stable at oxygen partial pressures ranging from above one atmosphere down to almost the dissociation pressure of the oxide. While there seems to be fairly good agreement that the surface is stoichiometric and Al-terminated (a relaxed bulk termination), the way the surface relaxes is not resolved yet. Experiments find an inward relaxation of 50%–60% for the outermost Al layer, while theoretical studies suggest something nearer 70%–80%. Discrepancies of this magnitude, amounting to 0.2–0.3 Å, are regarded as a serious test for theory and experiments. Calculations which included a monolayer of hydrogen[10] improved the situation somewhat, reducing the relaxation to 69%, but this is still rather more than experimental values, and furthermore in the most recent LEED study,[9] the authors suggest that their specimen preparation should have eliminated the hydrogen.

The $(01\bar{1}2)$ surface also received some attention, experimental with LEED[35] and Crystal Rod Truncation Diffraction[17] studies, as well as one partial electronic struc-

TABLE I. Surfaces energies of alumina, absolute and relative to the (0001) surface.

Face	Area (Å^2)	Experiment (Ref. 31) (relative)	Experiment (Ref. 32) (relative)	GGA, this work		LDA (Ref. 20)		Atomistic (Ref. 19)	
				(J m^{-2},	relative)	(J m^{-2},	relative)	(J m^{-2},	relative)
(0001)	19.53	1.00	1.00	1.98	1.00	1.76	1.00	2.42	1.00
$(01\bar{1}2)$	24.27	1.05	0.85	2.04	1.03	1.97	1.12	2.38	0.99
$(11\bar{2}3)$	40.50	1.06	0.96	2.25	1.13	···	···	2.84	1.18
$(11\bar{2}0)$	35.49	1.12	0.97	2.34	1.18	1.86	1.06	2.67	1.11
$(10\bar{1}0)$	61.46	1.16	1.01	2.56	1.29	1.40	0.80	2.86	1.19
$(10\bar{1}1)$	20.49	1.07	0.95	2.57	1.30	2.55	1.45	3.18	1.32
$(22\bar{4}3)$	73.61	···	···	2.77	1.40	···	···	3.07	1.27

ture work[21] (no relaxation allowed). In the recent CRTD study, Trainor *et al.* proposed two models, one stoichiometric, the other O terminated, and suggest that the latter one is more plausible. They also observe that water has little influence on their data. Our atomistic calculations can provide insight in the relative stability of these models, and help understand the role of water.

The $(11\bar{2}0)$ surface has also been investigated in details using of electronic microscopy,[36] TPD[37] and LEED and HAS.[16] There is evidence for a high-order commensurate phase for temperatures higher than 1400 K (the surface reconstruct in a (12×4) superstructure, which has lost 50% of the first layer oxygen), while the 1×1 phase is stable at lower temperature. It is found that the surface is totally unreactive to hydrogen adsorption (molecular and atomic).[16]

Finally, to the best of our knowledge the other surfaces have only been considered by ‘‘general’’ studies: Experimental with internal pore optical microscopy,[32] theoretical either with semiempirical models[19] or LDA.[20]

IV. RESULTS AND DISCUSSION

A. Stoichiometric surfaces

In Table I, we present our results for the stoichiometric surfaces, as well as those from the most recent of previous studies (albeit still limited to stoichiometric surfaces). One can find a more thorough list of calculated values in Table I of Ref. 32.

The corresponding morphologies are drawn in Fig. 1, as a guide and as a convenient way for direct comparison with internal pore optical microscopy results.

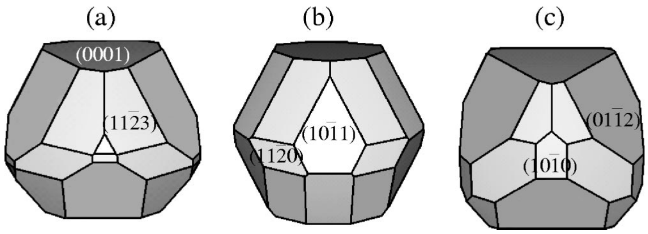

FIG. 1. Wulff shapes of alumina. (a) GGA, this work. (b) Internal pore optical microscopy (Ref. 31). (c) Shell model (Ref. 19).

Six surfaces appear in the calculated morphology of the stoichiometric: (0001), $(01\bar{1}2)$, $(11\bar{2}3)$, $(11\bar{2}0)$, $(10\bar{1}0)$, and $(10\bar{1}1)$.

While the two recent morphology oriented experimental work[31,32] are consistent, they obtain different surface energy sequences. In fact, the energy sequences differ mostly with respect to the basal (0001) surface. In one case[31] this surface is the most stable [with the $(01\bar{1}2)$ being second most stable], while in the other case[32] the $(01\bar{1}2)$ is the most stable and the (0001) is fifth most stable! Our results favor the former ordering.

The main difference between the GGA and the experimental Wulff shapes mostly concerns the surface energy of the $(10\bar{1}1)$ surface. It seems clear that calculation overestimates it (relative surface energy of 1.29, compared to 1.07 or even 0.95). In the absence of a structural experiment concerning this surface, one can only postulate that this surface could be stabilized by faceting, thus reducing its surface energy. Another possibility is that this surface adopts a different stoichiometry while the others stay stoichiometric, but we consider it rather unlikely (see next section).

As a consequence of our overestimation of the $(10\bar{1}1)$ surface energy, the $(10\bar{1}0)$ surfaces which does not seem to be present in the experimental morphology,[32] appears in the calculated ones (albeit not very significantly). Indeed, changing the surface energy of the $(10\bar{1}1)$ to $2.34\ \mathrm{J\,m^{-2}}$ (from $2.57\ \mathrm{J\,m^{-2}}$) leads to the disappearance of the $(10\bar{1}0)$ facet and a generally much better visual agreement between the calculated and experimental morphologies.

We suggest that either experimental work based on structure sensitive probes, or more detailed theoretical studies are required to resolve the problems posed by the $(10\bar{1}1)$ surface.

B. Non-stoichiometric surfaces

1. Generation strategy

The non-stoichiometric surfaces are generated at random from the stoichiometric termination by removing peripherals atoms [as in a temperature programmed desorption (TPD) experiment] and allowing the surface to relax. However, this

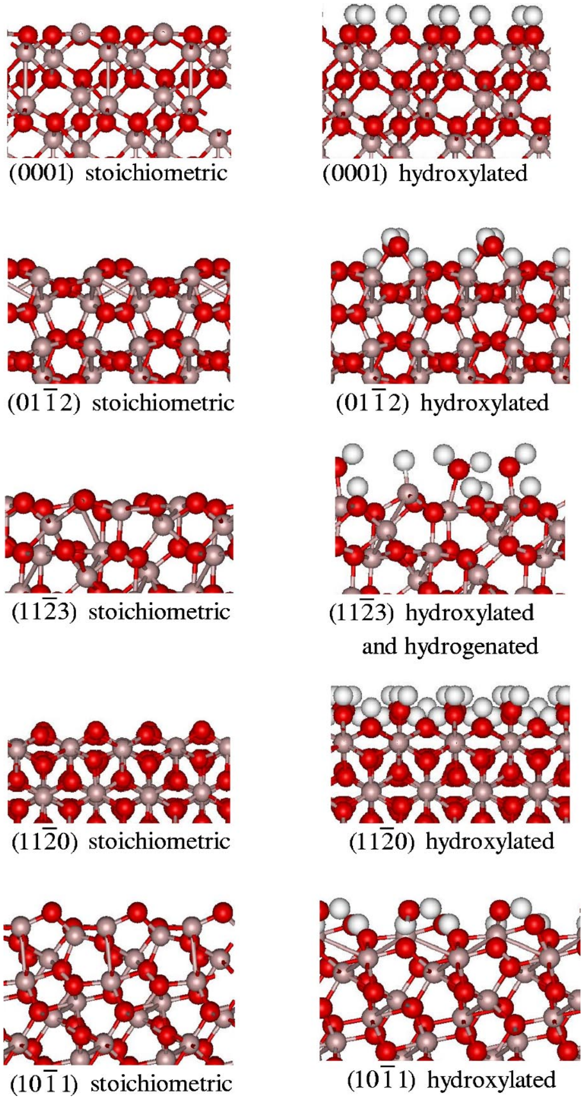
(0001) stoichiometric (0001) hydroxylated

$(01\bar{1}2)$ stoichiometric $(01\bar{1}2)$ hydroxylated

$(11\bar{2}3)$ stoichiometric $(11\bar{2}3)$ hydroxylated and hydrogenated

$(11\bar{2}0)$ stoichiometric $(11\bar{2}0)$ hydroxylated

$(10\bar{1}1)$ stoichiometric $(10\bar{1}1)$ hydroxylated

FIG. 2. Models of alumina surfaces. Dark gray for O, light gray for Al, and white for H.

still leaves many configurations to sample. Therefore, we also consider a second approach of using simple chemical rules, based on removing or adding species such as oxygen and hydrogen to the surface in order to maximize the number of atoms at their preferred coordination number or to test configurations appearing in various minerals. Up to 12 different configurations were considered for each surface, with the exception of the $(10\bar{1}0)$ which has a much bigger cell and which, coupled with its lack of appearance in experimental morphologies was neglected. The most stable configurations are presented in Fig. 2, mostly the stoichiometric and hydroxylated surfaces. Other configurations, containing different combinations of H and O (not necessarily in H_2O proportions) were of course simulated but are not all depicted in this figure. Even if Al rich environments are taken into account via the removal of peripherals O atoms we chose not to model highly reduced configurations such as the experimentally observed high temperature, $(\sqrt{31}\times\sqrt{31})$ reconstruction of the (0001) surfaces, because it is likely that the structure of the surface is strongly modified and that big supercells are needed to treat the reconstruction.

2. Phase stability

The surface energies of the different compositions and surfaces were calculated using the approach outlined above, from which we generate simple phase diagrams. Figure 3 contains the surface phase diagrams for each surface as functions of O and H chemical potential. The vertical lines represent the boundary for the O chemical potential as discussed in Sec. II B. The diagonal lines correspond to the water–H_2 equilibrium at different temperatures. Above these lines, H at the surface is in equilibrium with H_2O, under, with H_2.

If the phase diagrams are to be exploited one needs to relate the chemical potential to more pertinent variables. Figure 4 gives the pressure [Fig. 4(a)] and temperature [Fig. 4(b)] dependencies of the chemical potentials of oxygen and hydrogen (half the value of chemical potential of the corresponding diatomic, ideal gas species). We also plot the chemical potential of water as a function of temperature in Fig. 4(b), for further use. These curves were obtained using experimental data.[29,30]

The chemical potential of an ideal gas trivially varies monotonically with the corresponding partial pressure. The temperature dependence is slightly less obvious (as the correction to the standard chemical potential also depends on it), but in a reasonable range of pressure [below 10^7 bar, see H in Fig. 4(a)], the chemical potential decreases with temperature.

By converting the conditions of temperature and pressure into the corresponding chemical potential using Fig. 4, the phase diagrams of Fig. 3 can be employed to evaluate the most stable surface phase in a given environment.

The most significant result from the surface phase diagram of Fig. 3, is that in all but one case, only two types of surface can be found on alumina: Stoichiometric or fully hydroxylated. Other configurations, for instance O or OH adsorption or simple Al rich surfaces do not seem to be stable (we recall that we do not consider Al very-rich configurations, such as the $(\sqrt{31}\times\sqrt{31})$ reconstruction of the (0001) surfaces). Furthermore, the hydroxylated surfaces are those where the Al are sixfold coordinated and the O threefold coordinated. Thus the surfaces are formed by the addition of a few water molecules per unit cell to the stoichiometric surface, which results in the boundary between the two phases being parallel to the hydrogen–water equilibrium.

For a given surface, the water equivalent chemical potential $\mu^T = 2\cdot\mu_{\mathrm{H}} + \mu_{\mathrm{O}}$ is constant at the boundary between the two phases, the higher this value, the less stringent are the conditions for the surface to be stoichiometric. It might be clearer to represent this in terms of a water equilibrium equivalent temperature, chosen here at standard pressure [see Fig. 4(b)]. At this temperature, the surface would experience a phase transition (even if such a simple image does not convey any kinetic information). The higher this temperature, the wider is the range where the hydroxylated phase is more stable than the stoichiometric.

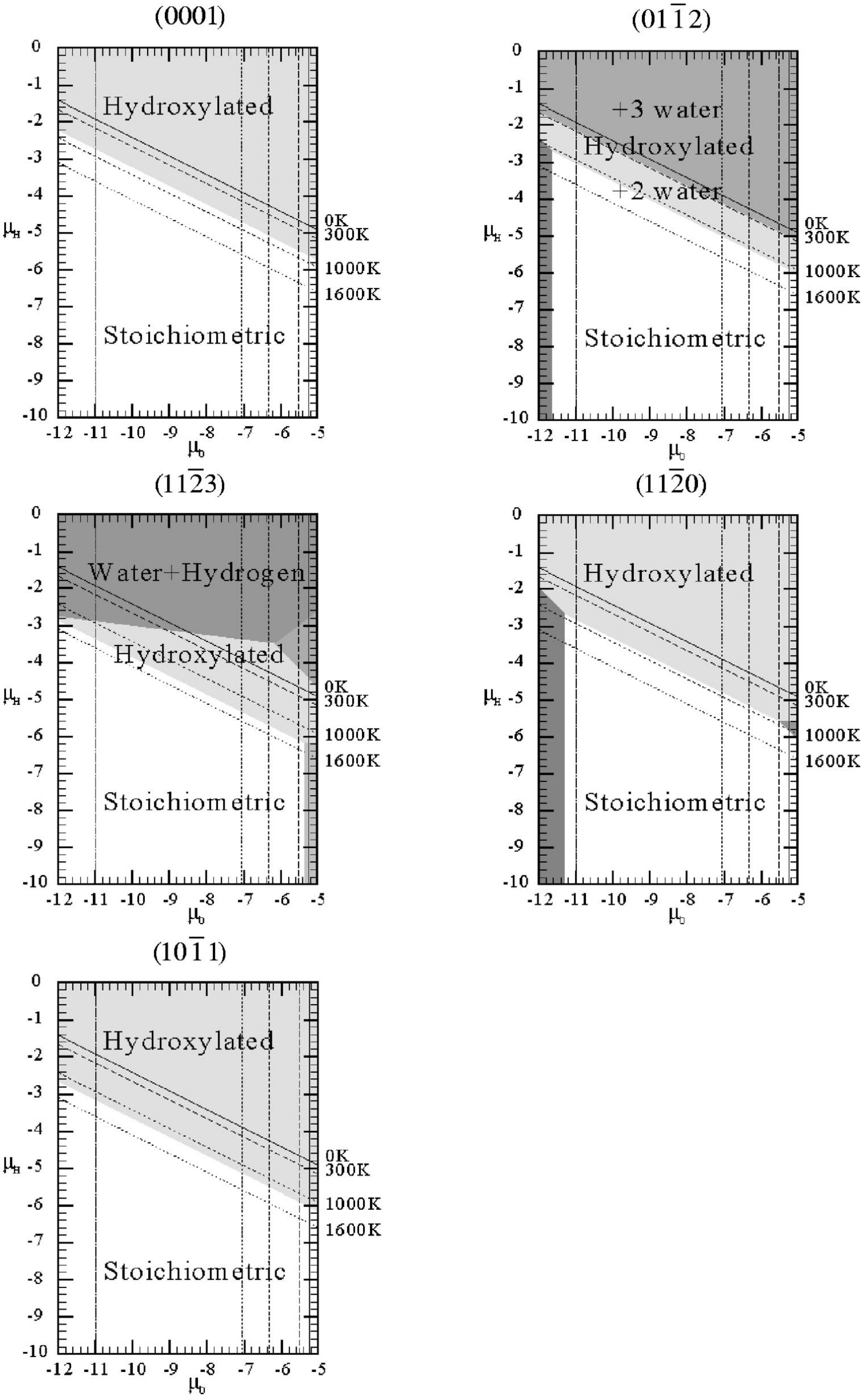

FIG. 3. Phase diagrams for alumina surfaces, (chemical potential in eV). White, stoichiometric termination, light gray, hydroxylated, other gray for other terminations. The vertical lines limit the stability domain of alumina. The diagonal ones correspond to the water–H_2 equilibrium.

Amongst the surfaces we studied, the $(11\bar{2}3)$ is the one for which hydroxylation is the more favorable, with a μ^T of -17.8 eV (1370 K) followed by $(10\bar{1}1)$ at -17.3 eV (1180 K), $(01\bar{1}2)$ at -17.1 eV (1090 K), $(11\bar{2}0)$ at -16.7 eV (920 K), and (0001) at -16.5 eV (840 K).

At the temperature at which the morphology experiments were conducted (1600 and 1800 K), we have little doubts that the surfaces are stoichiometric. Furthermore, the $(10\bar{1}1)$ surfaces, which is the one where our results differ the most with the experiments, is not the surface which would hydroxylate most readily, which is why we do not believe that non-stoichiometry can explain the discrepancy.

Within the oxide stability range, we find evidence of only one surface, which differs from the stoichiometric–

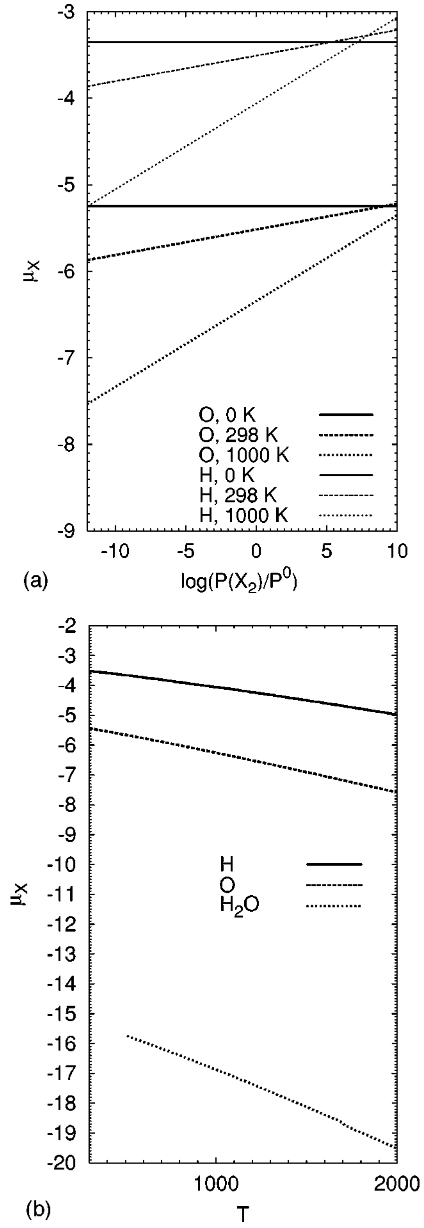

FIG. 4. Chemical potential (O, H, and H_2O) dependence on partial pressure (a) (for different temperature) and temperature (b) (at 1 bar).

hydroxylated pattern (also where Al adopts a different coordination). At high H_2 (or H_2O) partial pressure the $(11\overline{2}3)$ surface adopts a more complex structure where the last Al atom is fourfold coordinated (3 bonds with O atoms, 1 with an H atom) and with dissociated water molecules.

We attribute this dominance of stoichiometric or hydroxylated structures to the fact that Al prefers energetically not to change its oxidation state, as opposed to the cases of iron[38] or ruthenium[39] oxides for instance.

3. (0001) surface

As previously discussed, the (0001) surface has been very actively studied. Here we check the plausibility of our multisurface results by comparing various energetic and structural properties with earlier, similar studies[10–12] of the basal plane surface.

For the ubiquitous stoichiometric surface, we obtain a surface energy of $1.98\ \mathrm{J\cdot m^{-2}}$, in good accord with the previous studies (2.13,[10] 1.95,[11] and 1.98[12]). The relaxations of the first three layers (-84%, $+17\%$, -58%) concur with those obtained by DFT (-86%, $+6\%$, -49%),[10] (-70%, $+10\%$, -34%),[11] (-85%, $+3\%$, -45%),[12] and therefore, are quite different from those experimentally observed (-50%, $+6\%$).[7,9] The in-plane rotation of the surface O atoms has been measured[4] at 6.7°, but a previously calculated value[11] is only in qualitative agreement at 3.1°, as is ours at 1.9°.

All the aforementioned studies also agree that the O terminated surface can only be stabilized in the presence of hydrogen. We totally agree, as the hydroxylated phase of Fig. 3(a) can be described either as the result of the adsorption of three water molecules the stoichiometric O-terminated surface (of double the surface area, and much less stable than its Al terminated equivalent) or as the triple hydrogenation of the non-stoichiometric O-terminated surface.

The good concordance between our description of the basal surface and previous works suggests that the results on other, less studied surfaces, are equally valid.

4. $(11\overline{2}0)$ surface

The phase diagrams also allow us to reinterpret experimental data. For example, Becker *et al.* proposed that the $(11\overline{2}0)$ surface is unreactive towards molecular or even atomic hydrogen at room temperature. We find that, thermodynamically, at room temperature, even under ultrahigh vacuum (UHV) conditions, the equilibrium state of the surface is the fully hydroxylated one. We suggest that the lack of reactivity of molecular or atomic hydrogen with the surface is due to the fact that the surface under scrutiny is already terminated by H atoms. The authors ruled out this explanation on the basis that the (0001) surface was supposedly similar, and had been shown to experience a noticeable loss of hydrogen at 1400 K. Our results suggest that on thermodynamic grounds this analogy is questionable, as the (0001) and the $(11\overline{2}0)$ differ noticeably with respect to their affinity for hydroxylation (hydroxylated-stoichiometric transition at 920 K for the former, 840 K for the latter). Furthermore, the structure of the two hydroxylated surfaces is quite different (Fig. 2) and there is no guarantee that the kinetic effects likely to govern hydrogen desorption are comparable.

A further experimental result that should be investigated concerns the reconstructed (12×4) superstructure, but because of its size, it cannot be tested yet. However, we do not find that a surface with half its first layer oxygen missing (as a model for the (12×4)) is comparatively stable. Whether this is due to the size limit or to an incomplete sampling of the numerous different configurations cannot be resolved here. We plan to investigate this in a dedicated study.

5. $(01\overline{1}2)$ surface

According to CTRD measurements, two configurations are plausible for the $(01\overline{1}2)$ surface: A stoichiometric surface, and one where the aluminums of the first layer are missing. This last phase was investigated, but it does not appear to be stable in any area of the phase diagram. We should point out, however, that the fully hydroxylated surface (noted "+3 water" in Fig. 3), when stripped of its surface hydrogen atoms, corresponds to this experimental structure. It is worth mentioning here that this more hydroxylated surface corresponds to the addition of three water molecules per elementary area, not to the most stable stoichiometric cut (which can accept only two water molecules, "+2 water" in Fig. 3), but to another stoichiometric cut, significantly less stable (by $2.1\,\mathrm{J\,m^{-2}}$) when not hydroxylated. Keeping in mind that CTRD cannot directly observe the presence of hydrogen, we are confident that the structure observed by Trainor *et al.* is actually the fully hydroxylated one. This is further validated by the fact that the relaxations of the first four layers of the hydroxylated phase are in qualitative agreement: $(-48\%, +31\%, -11\%, +14\%)$ experimentally and $(-37\%, +60\%, -7\%, +25\%)$ from our results.

The fine details of the dynamics and structures of these last two surfaces are not relevant to this thermodynamic discussion and will be discussed in a companion paper.

V. SUMMARY AND CONCLUSIONS

We have calculated the surface energy of relevant alumina stoichiometric surfaces, using modern pseudopotentials and functionals. These energies are needed to update older sets of calculations, which had been requested in experimental studies. We find that the sequence of surface energy is closer to the results of Choi *et al.*[31] where the (0001) is clearly the most stable surface than to those of Kitayama *et al.*[32] The only real discrepancy between these experiments and our results concerns the $(10\bar{1}1)$ surface, which the simulation fails to identify as relevant to the crystal morphologies as it appears experimentally.

We also calculated the surface energy for many nonstoichiometric terminations of the previously mentioned surfaces, and discuss their stability with respect to partial pressure of hydrogen, water and oxygen and temperature, with the use of phase diagrams. For most of the surfaces, only the stoichiometric surface (low partial pressures, high temperature) and the hydroxylated (high pressures, low temperature) are predicted to be thermodynamically stable.

Finally, we suggest that the observed lack of reactivity of the $(11\bar{2}0)$ surfaces is due to the fact that the surface is already hydrogen terminated.

We also confirm the suspicion of Trainor *et al.* that of the two proposed structure for the $(01\bar{1}2)$ surface (relaxed bulk termination—stoichiometric- and Al poor) that their Al poor structure is in fact hydroxylated.

ACKNOWLEDGMENT

This work is supported by NERC.

---

*Electronic address: a.marmier@bath.ac.uk

†Electronic address: chsscp@bath.ac.uk

[1] K. Wefers and C. Misra, *Oxides and Hydroxides of Aluminium* (Alcoa Laboratories, 1987).

[2] V. E. Heinrich and P. A. Cox, *The Surface Science of Metal Oxides* (Cambridge University Press, Cambridge, 1994).

[3] J. Ahn and J. W. Rabalais, Surf. Sci. **388**, 121 (1997).

[4] P. Guenard, G. Renaud, A. Barbier *et al.* Surf. Rev. Lett. **5**, 321 (1998).

[5] G. Renaud, Surf. Sci. Rep. **32**, 1 (1998).

[6] J. Toofan and P. R. Watson, Surf. Sci. **401**, 162 (1998).

[7] C. F. Walters, K. F. McCarthy, E. A. Soares *et al.*, Surf. Sci. **464**, L732 (2000).

[8] T. Suzuki, S. Hishita, K. Oyoshi *et al.*, Surf. Sci. **437**, 289 (1999).

[9] E. A. Soares, M. A. Van Hove, C. F. Walters *et al.*, Phys. Rev. B **65**, 195405 (2002).

[10] X. G. Wang, A. Chaka, and M. Scheffler, Phys. Rev. Lett. **84**, 3650 (2000).

[11] I. G. Batyrev, A. Alavi, and M. W. Finnis, Phys. Rev. B **62**, 4698 (2000).

[12] R. Di Felice and J. E. Northrup, Phys. Rev. B **60**, R16287 (1999).

[13] Z. Lodziana, J. K. Norskov, and P. Stoltze, J. Chem. Phys. **118**, 11179 (2003).

[14] M. Baudin and K. Hermansson, Surf. Sci. **474**, 107 (2001).

[15] A. Marmier and M. W. Finnis, J. Phys.: Condens. Matter **14**, 7797 (2002).

[16] T. Becker, A. Birkner, G. Witte *et al.*, Phys. Rev. B **65**, 115401 (2002).

[17] T. P. Trainor, P. J. Eng, G. E. Brown *et al.*, Surf. Sci. **496**, 238 (2002).

[18] W. C. Mackrodt, R. J. Davey, S. N. Black *et al.*, J. Cryst. Growth **80**, 441 (1987).

[19] N. H. de Leeuw and S. C. Parker, J. Am. Ceram. Soc. **82**, 3209 (1999).

[20] I. Manassidis and M. J. Gillan, J. Am. Ceram. Soc. **77**, 335 (1994).

[21] J. Guo, D. E. Ellis, and D. J. Lam, Phys. Rev. B **45**, 13647 (1992).

[22] G. W. Watson, E. T. Kelsey, N. H. de Leeuw *et al.*, J. Chem. Soc., Faraday Trans. **92**, 433 (1996).

[23] G. Kresse and J. Furthmuller, Phys. Rev. B **54**, 11169 (1996).

[24] G. Kresse and J. Furthmuller, Comput. Mater. Sci. **6**, 15 (1996).

[25] G. Kresse and J. Hafner, Phys. Rev. B **49**, 14251 (1994).

[26] G. Kresse and J. Hafner, Phys. Rev. B **47**, 558 (1993).

[27] D. Vanderbilt, Phys. Rev. B **41**, 7892 (1990).

[28] G. Kresse and J. Hafner, J. Phys.: Condens. Matter **6**, 8245 (1994).

[29] *CRC Handbook of Chemistry and Physics* (CRC Press, Boca Raton, FL, 1981).

[30] H. Y. Afeefy, J. F. Liebman, and S. E. Stein, in *NIST Chemistry WebBook, NIST Standard Reference Database Number 69*, edited by P. J. Linstrom and W. G. Mallard (National Institute of Standards and Technology, Gaithersburg MD, March 2003).

[31] J. H. Choi, D. Y. Kim, B. J. Hockey *et al.*, J. Am. Ceram. Soc. **80**, 62 (1997).

[32] M. Kitayama and A. M. Glaeser, J. Am. Ceram. Soc. **85**, 611 (2002).

[33] J. R. B. Gomes, I. D. R. Moreira, P. Reinhardt *et al.*, Chem. Phys. Lett. **341**, 412 (2001).

[34] I. Batyrev, A. Alavi, and M. W. Finnis, Faraday Discuss. **114**, 33 (1999).

[35] M. A. Schildbach and A. V. Hamza, Surf. Sci. **282**, 306 (1993).

[36] T. Hsu and Y. T. Kim, Surf. Sci. **243**, L63 (1991).

[37] M. A. Schildbach and A. V. Hamza, Phys. Rev. B **45**, 6197 (1992).

[38] X. G. Wang, W. Weiss, S. K. Shaikhutdinov *et al.*, Phys. Rev. Lett. **81**, 1038 (1998).

[39] K. Reuter and M. Scheffler, Phys. Rev. B **65**, 035406 (2002).